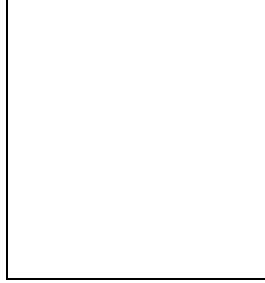


DETERMINATION OF NEUTRINO MASSES, PRESENT AND FUTURE

J.-L. Vuilleumier

Institut de physique, A.-L. Breguet 1, CH-2000 Neuchâtel, Switzerland



Oscillation experiments show that neutrinos have masses. They however only determine the neutrino mass differences. Information on the absolute masses can be obtained by studying the kinematics in weak decays, or by searching for neutrinoless double beta decay. Recent results are reviewed, as well as future projects.

1 Introduction

The lagrangian for the neutrinos may contain Dirac mass terms m^D , as for all other particles. In addition, Majorana mass terms m^L and m^R for left respectively right handed neutrinos, can appear:

$$\mathcal{L} = \sum_{\ell, \ell'} (m_{\ell\ell'}^D \bar{\nu}_{\ell L} \nu_{\ell' R} + m_{\ell\ell'}^L \bar{\nu}_{\ell R}^c \nu_{\ell' L} + m_{\ell\ell'}^R \bar{\nu}_{\ell L}^c \nu_{\ell' R}) + h.c.$$

The Dirac mass terms conserve the total lepton number ($\Delta L = 0$), while the Majorana terms break it by two units ($\Delta L = 2$). With them lepton number violating processes such as neutrinoless double beta ($\beta\beta 0\nu$) decay may occur. In any case the mass matrices are not in the most general case diagonal in the flavor ℓ ($\ell = e, \mu, \tau, \dots$). The flavor eigenstates ν_ℓ are then, assuming N generations of neutrinos, superpositions of $2N$ Majorana mass eigenstates ν_i with mass m_i . With Dirac mass terms only this reduces to a sum extending over N Dirac mass eigenstates ν_i :

$$\nu_\ell = \sum_{i=1}^N U_{\ell i} \nu_i.$$

and the flavor eigenstates ν_ℓ are Dirac as well. This equation also holds in the case of Majorana mass terms only. All eigenstates are then Majorana, with ν_ℓ representing the left handed Majorana flavor eigenstates.

With an off-diagonal mass matrix, neutrinos will undergo oscillations and transitions. With Dirac mass terms only, or Majorana mass terms only, because of the last equation, the oscillations or transitions take place between flavor eigenstates only.

Oscillation experiments are sensitive to the mixings $U_{\ell i}$ and the squared mass differences

$$\Delta m_{ik}^2 = m_i^2 - m_k^2.$$

Experiments with solar neutrinos determine a value $\Delta m_{sol}^2 \sim 5 \cdot 10^{-5} \text{ eV}^2$ and a large, but not maximum, mixing¹. Atmospheric neutrino experiments yield a second mass squared difference $\Delta m_{atm}^2 \sim 2.5 \cdot 10^{-3} \text{ eV}^2$ and a mixing consistent with the maximal value². These experiments cannot however determine the absolute masses.

This article is devoted to two other types of experiments providing informations on the absolute masses. First is the study of the kinematics in weak decays, such as ${}^3\text{H} \rightarrow {}^3\text{He} + e^- + \bar{\nu}_e$. These measure directly, in principle, the mixings $U_{\ell, i}$ and the masses m_i . And then additional information can be gained by studying $\beta\beta 0\nu$ decay, which measures an effective mass, exactly zero with Dirac masses alone, and taking the shape:

$$|\langle m_\nu \rangle| = \left| \sum_{i=1}^N U_{ei} U_{ei} m_i \right|$$

with Majorana masses alone.

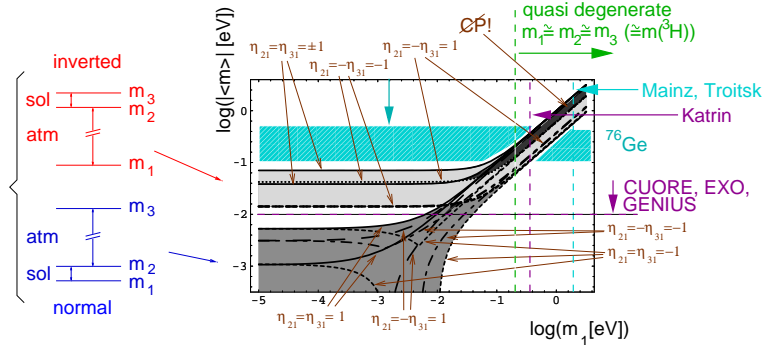


Figure 1: Region allowed by oscillation experiments in the $\langle m_\nu \rangle$ (effective double beta decay mass) vs. m_1 (lightest neutrino mass). Existing limits and projected sensitivities are indicated.

Moreover it must be mentioned that the study of cosmic microwave background (CMB) anisotropies and large scale structure (LSS) surveys of galaxies constrain the sum of all light neutrino masses. Relic Big-Bang neutrinos with too large masses would wash out these structures. A careful study of the CMB anisotropies measured by the WMAP satellite and of the 2dFGRS survey, assuming three neutrino families ($N = 3$), yields the limit $\sum_{i=1}^3 m_i < 2.12 \text{ eV}$ at 95 % CL³. It can be brought down to 1.01 eV by including additional input from cosmology.

The solar and atmospheric data are described well with three neutrino families. In that case, and assuming pure Majorana masses, the effective mass reduces to

$$|\langle m_\nu \rangle| = |m_1 |U_{e1}|^2 + m_2 |U_{e2}|^2 e^{i\alpha_{21}} + m_3 |U_{e3}|^2 e^{i\alpha_{31}}|,$$

where α_{21} and α_{31} are CP violating phases^{4,5}. In case of CP conservation they are such that

$$\eta_{21} = e^{i\alpha_{21}} = \pm 1, \quad \eta_{31} = e^{i\alpha_{31}} = \pm 1.$$

The aforementioned solar and atmospheric neutrino data, with their uncertainties, constrain two of the mixings, and the two squared mass differences. The third mixing is constrained by

the Chooz reactor experiment⁶. All this, for a given mass scale, usually taken as the mass m_1 of the lightest neutrino, constrains in turn the allowed range of $|\langle m_\nu \rangle|$ ^{4,5,7}. This is illustrated in fig. 1, taken from ref. ⁵, where the allowed regions in the $|\langle m_\nu \rangle|$ vs. m_1 plane are shown. For m_1 above 0.1 eV, the mass differences are small compared to the absolute masses. It is the quasi degenerate region. All masses take nearly the same value ($m_1 \simeq m_2 \simeq m_3$), which is the quantity measured in kinematic experiments. Because of possible cancellations, depending on the CP-phases, $|\langle m_\nu \rangle|$ can be smaller than m_1 , by about a factor 5. For m_1 below 0.01 eV the mass differences become large compared to m_1 itself. Here one distinguishes two scenarios. In the first one, corresponding to the normal hierarchy, solar neutrinos oscillate between the two light neutrinos, and atmospheric neutrinos between a light and a heavy one. In that case $|\langle m_\nu \rangle|$ is always less than 10^{-2} eV. In the second scenario, corresponding to inverse hierarchy, the solar neutrinos oscillate between the heavy neutrinos, and atmospheric neutrinos between a heavy one and the light one. With this, $|\langle m_\nu \rangle|$ is always larger than 10^{-2} eV.

The study of double beta decay and of the kinematics in weak decays thus gives the possibility to discriminate between these scenarios, and to fix the absolute mass scale. In particular, if m_1 is less than 0.01 eV, double beta decay can find out about the hierarchy, normal or inverted. For this it is however necessary to push the sensitivity down to the 0.01 eV level. Even if one can hope that ongoing and future oscillation experiments, in particular Kamland⁸, will further constrain the allowed areas in fig. 1.

In the following we are going to discuss existing bounds on neutrino masses, and look how far the sensitivity could extend in next generation experiments.

2 Kinematics in weak decays

2.1 Electrostatic spectrometers

For many years the best limits on the mass of the neutrino admixed most to the electron neutrino have come from the study of tritium decay ${}^3\text{H} \rightarrow {}^3\text{He} + e^- + \bar{\nu}_e$ with an end-point energy of $E_0=18.6$ keV. One looks for a distortion of the beta spectrum near the end-point due to the masses, as described in more details in ref. ⁹. Here the important parameters are high energy resolution, large acceptance since only a tiny fraction of the emitted electrons fall in the region of interest, and low background. The source must be such as to minimize energy losses. Presently the best results come from integral electrostatic spectrometers, built and operated in Troitsk¹⁰ and Mainz¹¹. These instruments consist in two superconducting coils, generating a magnetic field, as shown in fig. 2. The source is placed at the entrance of one of the coils. The electrons emitted in the forward half-sphere spiral toward the detector, located behind the second coil. As they move to regions with a weaker magnetic field, the transverse momentum changes into longitudinal motion. Electrodes are used to create an electric potential barrier U . Only electrons with an energy above eU can pass the barrier, and are accelerated toward the detector. Scans are performed varying the potential U , providing the integral electron spectrum. The energy resolution is given by

$$\frac{\Delta E}{E} = \frac{B_{min}}{B_{max}}.$$

The Troitsk device uses a gaseous ${}^3\text{H}_2$ source, which has the advantage of minimal energy losses. The energy resolution is 3.5 eV. Early spectra showed an anomaly near end points, fits with one single mass yielding a negative squared mass. This is now believed to be due to an experimental artifact, and was eliminated in the most recent spectra. Older data are necessary however to minimize the statistical errors. The negative squared mass can be eliminated by adding in the fit a step to the integral spectrum, ending at an energy below E_0 , which was found

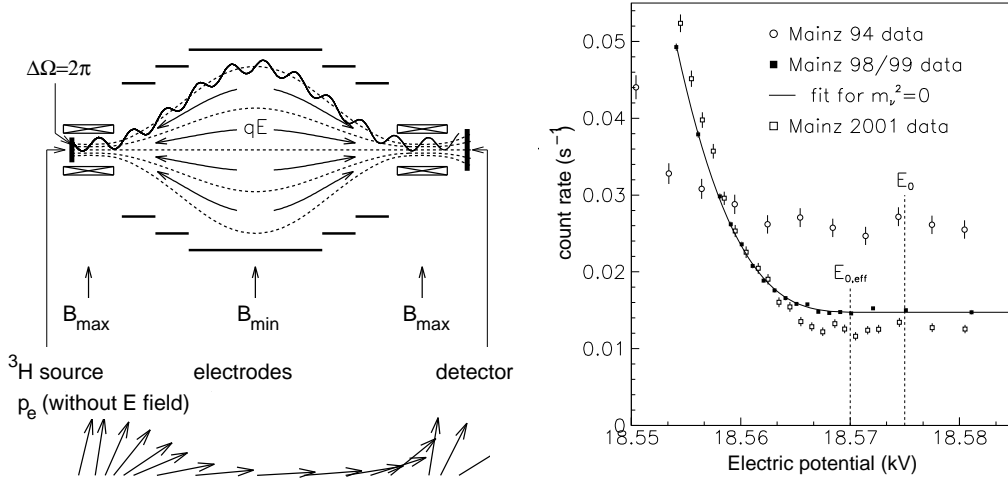


Figure 2: Left: principles of operation of an integral electrostatic spectrometer; evolution of the momentum of an electron spiraling in the magnetic field for no electric field; right: the Mainz ${}^3\text{H}$ spectra near end-point.

to vary in time. With this a negative squared mass consistent with zero is obtained, leading to the limit $m_\nu < 2.2$ eV at 95 % CL.

The Mainz system has an energy resolution of 4.8 eV. It uses a frozen ${}^3\text{H}_2$ source. The experiment went through several upgrades, which led in particular to a lower background, as shown in fig. 2. Distortions leading here also to negative squared masses were understood as being due to a roughening of the source film and were eliminated by substantially reducing the operating temperature. The last years of operation give a negative squared mass consistent with zero, and to the same limit

$$m_\nu < 2.2 \text{ eV at 95 \% CL,}$$

which can thus be considered presently the best upper bound on the neutrino mass, ruling out part of the quasi degenerate region in fig. 1.

The Mainz and the Troitsk groups consider that they have exhausted the potential of their instruments. They have joined efforts and, along with a few additional teams, have undertaken the construction of *Katrin*, a much larger device⁹. The energy resolution should be of order 1 eV. A small spectrometer will be placed in front of the main one, filtering out all the electrons clearly below the end-point, reducing the background considerably. A gaseous and a frozen ${}^3\text{H}$ source will be used, helping in pinning down the systematics associated with either source. With all this it is hoped that the sensitivity to the neutrino mass will extend down to 0.35 eV.

2.2 Bolometers

Cryogenic bolometers, proposed first by the Genova group, may turn out to be fairly competitive in searching for the neutrino mass.

In these, the source, in crystalline form, is the detector medium itself. The entire energy deposited by an event ends up in heat. The crystal is operated at low temperature, so that the corresponding temperature increase is large, and can be measured with a thermistor glued to the crystal. In principle, no corrections need to be made for final state or source effects.

The Genova group¹² has demonstrated the feasibility of using metallic rhenium crystals to look for the decay ${}^{187}\text{Re} \rightarrow {}^{187}\text{Os} + e^- + \bar{\nu}_e$ (natural abundance of ${}^{187}\text{Re}$ 62 %). One advantage is the low end point energy ($E_0 \simeq 2.5$ keV), which makes that a larger fraction of events falls in the region of interest. But the most recent results have been produced by the Milano group¹³.

An array of 10 AgReO₄ crystals with a mass of 250-300 μg each has been built and operated for a longer period of time. The measured spectra with and without calibration source are shown in fig. 3. The energy resolution is 28 eV on average at 2.5 keV. The measured spectrum was found to be in good agreement with a vanishing neutrino mass, and the limit $m_\nu < 21.7$ eV at 90 % confidence was derived. This is limited by statistics, and by the energy resolution. But clearly the method still has a lot of potential.

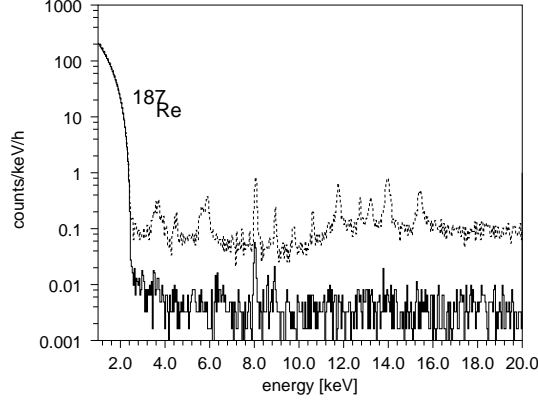


Figure 3: The ¹⁸⁷Re spectrum measured with the Milano bolometers, with and without calibration source.

3 Double beta decay

We are going to discuss neutrinoless and two neutrino nuclear double beta decay. The two neutrino mode $\beta\beta 2\nu (A, Z) \rightarrow (A, Z + 2) + e^- + e^- + \bar{\nu}_e + \bar{\nu}_e$ conserves the lepton number and is allowed in the standard model. The half life is given by

$$\left(T_{1/2}^{2\nu}\right)^{-1} = G^{2\nu}(E_0, Z) |M_{GT}^{2\nu}|^2$$

with $G^{2\nu}(E_0, Z)$ an exactly calculable phase space factor depending only on the nuclear charge Z and the total energy released in the decay E_0 , and $M_{GT}^{2\nu}$ a matrix element.

Neutrinoless double beta decay $\beta\beta 0\nu (A, Z) \rightarrow (A, Z + 2) + e^- + e^-$ breaks the lepton number by two units and requires Majorana masses. The half life depends directly on the effective mass $\langle m_\nu \rangle$:

$$\left(T_{1/2}^{0\nu}\right)^{-1} = G^{0\nu}(E_0, Z) \left| M_{GT}^{0\nu} - \frac{g_V^2}{g_A^2} M_F^{0\nu} \right|^2 |\langle m_\nu \rangle|^2,$$

with again $G^{0\nu}(E_0, Z)$ a phase space factor, g_V and g_A the vector and axial vector coupling constants, and $M_{GT}^{0\nu}$ and $M_F^{0\nu}$ matrix elements which are not the same as those of $\beta\beta 2\nu$, but which depend on the same nuclear physics.

Experimentally the two modes can be distinguished by measuring the total energy carried away by the two electrons. In ($\beta\beta 2\nu$) it follows a smooth distribution peaking at about $1/3 E_0$, while in ($\beta\beta 0\nu$) it is equal to E_0 . In either case the theoretical distributions are smeared by the instrumental resolution, as shown in figure 4. Many isotope candidates have been explored over the past years. The criterias of selection are high energy release E_0 , corresponding to a large phase space, and placing the search for $\beta\beta 0\nu$ decay in a region with lower background, and large natural abundance, which facilitates enrichment.

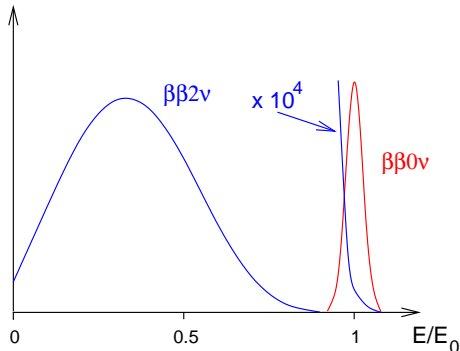


Figure 4: The expected energy distributions of the sum energy of the two neutrinos for $\beta\beta 0\nu$ and $\beta\beta 2\nu$ decay, smeared by energy resolution (gaussian with $\sigma(E)/E=2\%$).

	$T_{1/2}^{2\nu} meas.$ (yr)	$\frac{T_{1/2}^{calc}}{T_{1/2}^{meas}}$ QRPA ^{15,16}	$\frac{T_{1/2}^{calc}}{T_{1/2}^{meas}}$ Shell model ¹⁷
⁴⁸ Ca	$(4.2 \pm 1.2) \cdot 10^{19}$	—	0.91
⁷⁶ Ge	$(1.3 \pm 0.1) \cdot 10^{21}$	1.0	2.0
⁸² Se	$(9.2 \pm 1) \cdot 10^{19}$	1.3	0.40
¹⁰⁰ Mo	$(8 \pm 0.6) \cdot 10^{18}$	0.76	—
¹³⁰ Te	$(6.1 \pm 1.4 stat. \left(\begin{smallmatrix} +2.9 \\ -3.5 \end{smallmatrix} sys. \right)) \cdot 10^{20}$	0.36	0.38

Table 1: List of measured $\beta\beta 2\nu$ half-lives; comparison with QRPA and shell model predictions.

3.1 Present experiments

$\beta\beta 2\nu$ decay has now been seen in many nuclei⁷, as shown in table 1. The most recent entry comes from the Mibeta group, which built an array of 20 crystals of TeO_2 ¹⁴ of 340 g each, operated as bolometers at a temperature of 8 mK. The energy resolution is excellent, of order $\sigma(E)/E = 1.5 \cdot 10^{-3}$ at $E_0 = 2528$ keV. Most crystals use natural tellurium (34.5 % ¹³⁰Te). But recent measurements were performed with two of the crystals enriched in ¹³⁰Te, and two more enriched in ¹²⁸Te. The comparison yields a positive signal, corresponding to the half-life reported in table 1 for ¹³⁰Te, and in reasonable agreement with earlier geochemical results.

A comparison is made in table 1 with calculated half-lives, using nuclear matrix elements calculated in the framework of QRPA^{15,16}, and with the shell model¹⁷. Reasonable agreement is observed, at the level of a factor of 2 or better. This is particularly true of the QRPA results, which shows that the calculations are quite realistic. This encouraged the authors of ref.¹⁸ to go one step further, and to use the measured half-lives to fix more precisely the parameters of the QRPA model, and to use them to calculate the $\beta\beta 0\nu$ matrix elements. These calculations should be more reliable than older ones, and will be used in the following to interpret the data on $\beta\beta 0\nu$ decay in terms of $\langle m_\nu \rangle$. They tend to give masses slightly larger than older calculations.

Some results on $\beta\beta 0\nu$ decay are listed in table 2, and deduced effective masses $\langle m_\nu \rangle$ are given with the QRPA matrix elements of ref.¹⁸ and the shell model matrix elements of ref.¹⁷. They include those of the Heidelberg-Moscow collaboration in Gran Sasso, operating an array of 5 crystals of germanium (11 kg total mass) enriched to 87 % in ⁷⁶Ge, and operated as semiconductor devices, with an energy resolution of order $\sigma(E)/E = 0.7 \cdot 10^{-3}$ at $E_0 = 2039$ keV¹⁹. The advantage of such a good resolution to search for $\beta\beta 0\nu$, and also to identify the background, is illustrated in figure 5. As pointed out by the authors, the background is not flat, as naively believed previously, also in other experiments, but weak background peaks from ²¹⁴Bi activity (²³⁸U chain) are visible, in spite of the high radiopurity of the detector. The peak intensities

	$T_{1/2}^{0\nu}$ [yr] (90 % CL)	$\langle m_\nu \rangle$ [eV]	
		QRPA ¹⁸	shell model ¹⁷
⁷⁶ Ge	$(0.8 - 35) \cdot 10^{25}$	0.13 - 0.85	0.24 - 1.6
¹³⁰ Te	$> 2.1 \cdot 10^{23}$	< 3.6	$< -$
¹³⁶ Xe	$> 4.4 \cdot 10^{23}$	< 3.3	< 5.2

Table 2: Measurements of $\beta\beta 0\nu$ half-lives; Deduced effective neutrino mass $\langle m_\nu \rangle$.

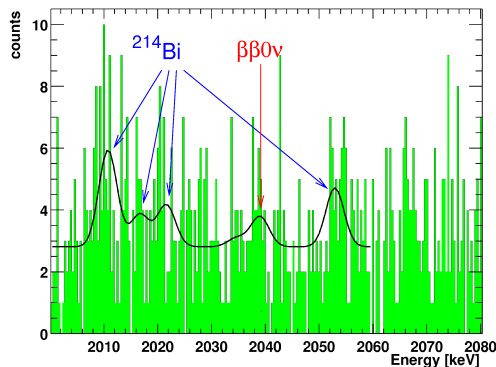


Figure 5: The $\beta\beta 0\nu$ energy region in the Heidelberg-Moscow ⁷⁶Ge data (55 kg-yr). The fitted background and $\beta\beta 0\nu$ peaks are shown.

are consistent with those of stronger ²¹⁴Bi peaks elsewhere in the spectrum. Fitting the region of interest with these peaks and a constant background, the authors find indications of an additional peak centered at $E_0 = 2039$ eV. They interpret this as an indication of $\beta\beta 0\nu$ decay, corresponding to a half-life of $T_{1/2}^{0\nu} = (0.8 - 35) \cdot 10^{25}$ yr (95 % CL). It would correspond to a mass $\langle m_\nu \rangle$ of order 0.1 to 1.6 eV, shown in fig. 1. This result has been the cause of heated debates, which will not be covered here. What is sure, is that $\langle m_\nu \rangle$ is less than 1.5 eV or so.

Other experiments at present can neither confirm nor disprove this indication, as shown in table 2. Given are the limits obtained with the already discussed Mibeta bolometers in ¹³⁰Te, and in ¹³⁶Xe with a xenon gas time projection chamber (TPC) operated in the Gotthard underground laboratory²⁰. Here the source consisted in 5.3 kg of xenon enriched to 62.5 % in ¹³⁶Xe. The philosophy was somewhat different. In comparison, the energy resolution is modest ($\sigma(E)/E = 2.5 \cdot 10^{-2}$ at $E_0 = 2480$ keV). But to a large extent this is compensated by the imaging capability of the TPC, a powerful tool to identify and suppress backgrounds, and to select double beta candidates, single continuous tracks with increased ionization due to larger dE/dx at both ends.

3.2 Future experiments

Clearly it is important to have improved data on $\beta\beta 0\nu$ decay, first to clear up the indication of the Heidelberg-Moscow ⁷⁶Ge experiment, and second to extend the sensitivity down to $\langle m_\nu \rangle \simeq 10^{-2}$ eV. NEMO 3 which has just started taking data in the Fréjus underground laboratory should be able to perform the first task²¹. It consist in a tracking detector with excellent imaging capability. In contrast to the detectors discussed so far, the source is not the detector medium. It is a thin foil, placed inside a fiducial volume filled with helium. This has the advantage that many nuclei can be investigated, but the disadvantage of energy losses in the source, deteriorating the energy resolution. Nevertheless with a source mass of 7 kg of molybdenum highly enriched in ¹⁰⁰Mo, and 1 kg of selenium enriched in ⁸²Se, it should probe $\langle m_\nu \rangle$ down to 0.1 eV or so.

Majorana	500 kg ^{76}Ge , 210 crystals in cryostats, segmented readout
MOON	34 t ^{nat}Mo sheets between plastic scintillators
XMASS	10 t of liquid ^{nat}Xe viewed by photomultipliers
CUORE	760 kg $^{nat}\text{TeO}_2$ bolometers
GENIUS	1(10)t of ^{76}Ge , in crystals suspended in liquid nitrogen
EXO	1(10)t of ^{136}Xe , in gas or in liquid TPC, with ion tagging

Table 3: Future projects to study $\beta\beta 0\nu$ decay, with brief description.

But more ambitious projects are required to go to 10^{-2} eV. The requirements on future detectors are much larger masses, of order 1, possibly 10 t, and, at the same time, much lower background level.

Masses of that kind can be envisioned, since highly efficient enrichment facilities exist in Russia, based on a variety of techniques, in particular centrifugation for components which can be brought to a gaseous form²². The reduction in background level which must go along can be achieved by the use of detector components with lower levels of natural and cosmogenic activities, improved event signature, and finally superior energy resolution.

Energy resolution is in any event essential since it is, practically, the only way allowing to suppress the background from $\beta\beta 2\nu$ decay when looking for $\beta\beta 0\nu$ decay. The experiments being considered will search for $\beta\beta 0\nu$ half lives of order 10^{26} to 10^{28} yr, longer by 5 to 7 orders of magnitude comparing with $\beta\beta 2\nu$ decay, as depicted in fig. 4. The differences in angular distributions can help, but not to the same extent. This favors detectors in which the source is at the same time the detector medium.

Several projects are being considered, some as general purpose detectors for low energy physics, including the study of solar neutrinos or the search for cold dark matter, others being primarily dedicated to double beta decay. Table 3 gives a non exhaustive list. In the following we will briefly discuss three of the projects, which will start on a smaller scale, before evolving to the final form.

CUORE is a development of Mibeta²³. It will consist in an array of 1000 crystals of $^{nat}\text{TeO}_2$, with a mass of 760 g each, operated as bolometers in a single low background cryostat in the Gran Sasso underground laboratory. The energy resolution should be better than $2\cdot 10^{-3}$ at $E_0 = 2480$ keV. An elaborate shielding made from roman lead, copper and PET should protect the crystals against local activities. It is hoped that the sensitivity to $\beta\beta 0\nu$ decay will extend up to half-lives of order $2\cdot 10^{26}$ yr, corresponding to roughly 0.1 eV in terms of the effective mass $\langle m_\nu \rangle$, or somewhat better.

In a first step a smaller version, CUORICINO, is being built in the Gran Sasso laboratory. It will have 56 crystals similar to those foreseen for CUORE.

GENIUS has been proposed by the Heidelberg group²⁴. It uses germanium crystals highly enriched in ^{76}Ge operated as semiconductor detectors, as in the Heidelberg-Moscow experiment. But to simplify the design, and reduce the possibility of radioactive contamination, the crystals are not mounted in a cryostat, but suspended and immersed in a large vessel filled with liquid nitrogen, as shown in fig. 6. Tests have shown that the excellent energy resolution inherent to semiconductor detectors can be maintained in such an arrangement. The FET's of the crystals, a source of background, can be mounted at a large distance. The liquid nitrogen can be cleaned to a high level of purity, and provides the innermost shielding layer against outside activities. Because of the low density, a large volume is required. Pulse shape discrimination will be used, as in the later phase of the Heidelberg-Moscow experiment, to distinguish single site events, potential double beta candidates, from multiple site events, mostly due to multiple Compton scattering. For the same reason the crystals will be operated in anti-coincidence. Careful background estimates have been performed, taking into account cosmogenic activation, leading

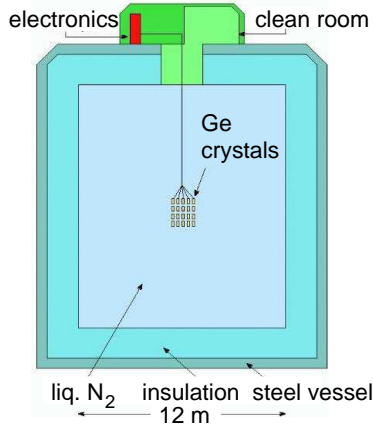


Figure 6: The proposed Genius detector with germanium crystals suspended in a liquid nitrogen bath.

to encouragingly low rates. The experiment should reach a sensitivity of order 10^{-2} eV or so to $\langle m_\nu \rangle$. A test facility, with 40 kg of natural germanium, is being set up at Gran Sasso.

EXO is devoted to the search of double beta decay in ^{136}Xe ²⁵. To reduce drastically the background the detector will have a much improved signature. It will be made so as to observe not only the two electrons emitted in double beta decay, as usual, but also to identify the positive ion left behind, in this case $^{136}\text{Ba}^{++}$ ²⁶. It is first brought to the singly charged state $^{136}\text{Ba}^+$. A first 493 nm laser brings it from the $6^2S_{1/2}$ ground state to the $6^2P_{1/2}$ excited state. From there it decays back to the ground state, or to the $5^4D_{3/2}$ metastable state. If this happens, a second 650 nm laser brings it back to the $6^2P_{1/2}$ state. As long as the laser irradiation continues, photons are emitted, which allow to identify the ion. R&D is in progress to develop this technique.

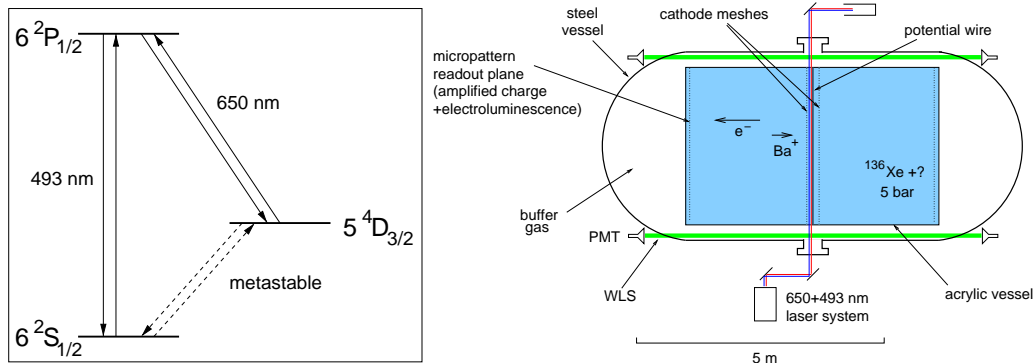


Figure 7: Left: The level scheme of $^{136}\text{Ba}^+$; right: a possible layout for the gas version of the EXO TPC (1 t).

Two options are being studied for the EXO detector. In either case the source consists of xenon highly enriched in ^{136}Xe and acting as detection medium for the electrons. The first possibility is a liquid TPC, which has the advantage of being compact and easy to shield. After the detection of the electrons, by measuring both the scintillation light and the ionization charge, the much slower positive ion is extracted with a tip at a negative potential. It is released in an ion trap by reversing the potential. The ion tagging is then performed in the trap.

A second possibility is a gas TPC, as in the Gotthard experiment. A disadvantage is the larger size of the detector. But the advantage is that the electron tracks are then long enough to be visualized. This provides a powerful additional selection criterion. The ion tagging must then be made in the TPC itself, a quencher admixed to the xenon bringing the ion from the doubly to the singly ionized state. A possible layout is shown in fig. 7, resembling that of MUNU ²⁷.

The TPC is enclosed in an acrylic vessel. The ionization electrons drift to the read-out planes, at both ends. The positive ion drifts much more slowly toward the cathode in the center, near which it crosses the laser beams. The desexcitation light is converted to green in wavelength shifter bars, and brought to photomultipliers at the ends.

Ion tagging, if it can be made to work efficiently, will lead to an essentially background free double beta decay experiment. But an energy resolution of order 2 % or better is necessary to distinguish $\beta\beta 0\nu$ decay from $\beta\beta 2\nu$ decay. This is only marginally better than what was achieved in the Gotthard experiment however, and R&D is in progress for both versions to improve on that²⁸. A first test experiment will be performed with 50 kg of enriched xenon, but without tagging. The next goal is an experiment with 1 t, having a sensitivity of a few 10^{-2} eV to $\langle m_\nu \rangle$. A 10 t version could, ultimately, be envisioned.

4 Conclusion

Next generation laboratory experiments studying the kinematics in weak decays and searching for neutrinoless double beta decay will further constrain neutrino masses. They should provide enough information to figure out what scenario holds for neutrino masses: nearly degenerate, inverted hierarchy or normal hierarchy.

These experiments are real challenges, facing many difficulties, in particular fierce background problems. They will thus proceed in several steps, before reaching the final sensitivity.

1. K. Heeger, these proceedings; the SNO collaboration, Phys.Rev.Lett. 89 (2002) 011302
2. J. Kameda, these proceedings; the Super-Kamiokande collaboration, Phys.Rev.Lett. 85 (2000) 3999
3. S. Hannestad, astro-ph/0303076, 2003
4. S. M. Bilenky, S. Pascoli and S. T. Petcov, Phys.Rev. D 64 (2001) 053010
5. S. Pascoli and S. T. Petcov, Phys.Lett. B 544 (2002) 239-250
6. M. Apollonio, Eur.Phys.J. C27 (2003) 331
7. Steven R. Elliott, Petr Vogel, Ann.Rev.Nucl.Part.Sci. 52 (2002) 115
8. The Kamland collaboration (K. Eguchi et al.), Phys.Rev.Lett. 90 (2003) 021802
9. C. Weinheimer, hep-ex/0210050
10. V. M. Lobashev et al., Phys. Lett. B 460 (1999) 227
11. J. Bonn et al., Nucl. Phys.(Proc. Suppl.) 91 (2001) 273
12. M. Galeazzi et al., Phys. Rev. C 63 (2001) 014302
13. C. Arnaboldi et al., submitted to Phys. Rev. Lett., hep-ex/0302006
14. C. Arnaboldi et al., Phys.Lett. B 557 (2003) 167
15. J. Engel et al., Phys. Rev. C 37 (1988) 731
16. M. Moe and P. Vogel, Ann. Rev. Nucl. Part. Sci., 44 (1994) 247
17. E. Caurier et al., Phys. Rev. Lett. 77 (1996) 1954; see also P. Vogel, nucl-th/9904065
18. V. A. Rodin et al., nucl-th/0305005, 2003
19. H.V. Klapdor-Kleingrothaus, A. Dietz and I.V. Krivosheina, Found.Phys. 32 (2002) 1181-1223, hep-ph/0302248
20. R. Luescher et al., Phys. Lett. B 434 (1998) 407
21. A.I.Etiennevre, these proceedings; R. Arnold et al., Nucl.Instrum.Meth. A 503 (2003) 649
22. P. K. Lebedev and V. I. Pryanichnikov, Nucl. Inst. and Meth. A 327 (1993) 222
23. C. Arnaboldi et al., hep-ex/0212053, 2003
24. H. V. Klapdor-Kleingrothaus et al., MPI Report MPI-H-V 26 1999; hep-ph/9910205
25. M. Danilov et al., Phys.Lett. B 480 (2000) 12
26. M. Moe, Phys. Rev. C 44 (1991) R931
27. The MUNU collaboration (M. Avenier et al.), Nucl.Instrum.Meth. A 482 (2002) 408
28. E. Conti et al., submitted to Phys. Rev. B; hep-ex/0303008